SIMULATING THE IMAGE CHAIN OF THE EXOMARS 2020 ROVER PANCAM WIDE ANGLE CAMERAS. R. B. Stabbins[1,2], A. D. Griffiths[1,2], A. J. Coates[1,2], M. Gunn[3], C. Huntly[3], F. Trauthan [4], N. Schmitz[4] and the PanCam Science Team [1]Mullard Space Science Laboratory, University College London, Holmbury St. Mary, Dorking, Surrey, RH5 6NT, UK (roger.stabbins.10@ucl.ac.uk), [2]Centre for Planetary Science at UCL/Birkbeck, University College London, Gower Street, Gower Street, London, WC1E 6BT, UK, [3]Department of Physics, Aberystwyth University, [4]Institute for Planetary Research, German Aerospace Centre (DLR), Berlin, Germany.

Introduction: The PanCam instrument [1] is a mast-mounted imaging system for the ExoMars 2020 rover [2], providing panoramic VNIR imaging for geological context, operations planning, and atmospheric science. The system consists of a stereo pair of wide angle cameras (WACs), enabling 3D scene reconstructions of local morphology, with a multispectral filter suite for composition studies of the surface and atmosphere. A high-resolution camera (HRC) positioned between the WACs allows for fine detail colour imaging.

We present a simulation of the PanCam WAC imaging system from component level information, to model the image formation process, including nonlinear response, and a comprehensive set of noise sources. A linear shift variant transfer function of the optics is computed for each pixel viewing angle, from measurements made on duplicate filter sets and from manufacturer supplied information of the lens assembly.

PanCam WAC Description: Each WAC consists of a 38.3ºx38.3º FoV f/10 lens stationed behind an 11 position filter wheel and a protective window. Of the 22 filters (total), there are 12 narrowband geology filters spanning 440nm-1000nm (6 per WAC) [3], 2 triplets of RGB broadband filters, and 4 low-transmission narrowband solar filters (2 per WAC). At the focal plane of the fixed focus optics, a Star 1000 CMOS APS detector is positioned, with a 1024x1024 array and 10-bit Analog-Digital Convertor (ADC). A comprehensive description of PanCam can be found in [1].

Camera Model: The system is modelled in two parts. First, an optics function transforms the directional distribution of light entering the aperture into an image at the focal plane, subject to the selected filter. A detector function then transforms the irradiance image into the 10-bit digital image output, subject to the exposure settings and detector temperature.

Optics Function. Eq. 1 translates the scene spectral radiance $\boldsymbol{R}(\lambda)$ to the spectral irradiance $\boldsymbol{I}(\lambda)$ incident on the detector, according to the camera equation and cosine falloff for incident angle $\boldsymbol{\alpha}$. The transmission functions of the selected filter and lens $\boldsymbol{\tau}_f(\lambda)\boldsymbol{\tau}_l(\lambda)$ then apply spectral attenuation to the signal.

$$\boldsymbol{I}(\lambda) = \frac{\pi}{4f\#^2}\cos^4(\boldsymbol{\alpha})\boldsymbol{\tau}_f(\lambda)\boldsymbol{\tau}_l(\lambda)\boldsymbol{R}(\lambda) \quad (1)$$

Due to the wide FoV, this function does not assume uniform spectral transmission across the field, as could be assumed for the relatively narrow FoVs of previous lander imaging systems (<19º H-FoV [4]).

Detector Function. The irradiance image cube is evaluated by eq. 2, giving an image in units of electrons accumulated per pixel well. This incorporates the conversion of radiation to photon flux, scaling over pixel area A_p, and photon-electron conversion by Quantum Efficiency function $QE(\lambda)$, and integration over exposure time t_e. The photo-response nonuniformity Q_{PR} applies a normally distributed fixed-pattern, accounting for variance in conversion efficiency. Additive noise sources of thermally generated dark signal $\boldsymbol{I}_d(T)$ and reset noise $\boldsymbol{E}_{kTC}$ are modelled. The temperature dependence of these noise sources is significant for the case of PanCam, as the detector temperature will be subjected to the thermal cycles of the martian surface. The dark signal nonuniformity quality factor $\boldsymbol{Q}_{DS}$ is distributed Log-Normally, with an additional uniform distribution describing the hot pixel population [5]. A convolution of the electron image with a 3x3 matrix $\boldsymbol{E}_x$ describing cross-talk between neighbouring pixels is then performed. Poisson counting statistics are applied to model detection shot noise, denoted by $\mathcal{P}(.)$.

$$\boldsymbol{E} = \begin{matrix}\mathcal{P}\left(t_e\boldsymbol{Q}_{PR}\frac{A_p}{hc}\int \boldsymbol{I}(\lambda)QE(\lambda)\lambda d\lambda\right) \\ + \mathcal{P}(t_e\boldsymbol{Q}_{DS}\boldsymbol{I}_d(T)) + \boldsymbol{E}_{kTC}\end{matrix} \otimes \boldsymbol{E}_x \quad (2)$$

The conversion gain G_{SN} (units of V/e-) of the CMOS 3T sense node is modelled by equation (3). Whilst CCD sensors (as used by previous lander imagers [4]) have a near linear response function, with a scalar G_{SN}, the Star 1000 CMOS APS sensors used for each of the 3 PanCam detectors are nonlinear, and so require a signal dependent function $G_{SN}(\boldsymbol{E})$.

This semi-empirical equation has been formulated to depend on the pixel Full Well charge E_{FW}, linear conversion gain G_{Lin}, saturation voltage V_{Sat}, and tuning parameters *a* and *b*.

$$G_{SN}(\boldsymbol{E}) = \frac{V_{Sat}\text{-}a}{1 + exp\left(\text{-}bG_{Lin}(\boldsymbol{E}\text{-}E_{FW})\right)} + G_{Lin}\boldsymbol{E} \qquad (3)$$

The final stage amplifies the resultant voltage signal according to the Star 1000 FPGA amplifier settings, applying offset column pattern noise $\boldsymbol{O}_{CPN}$. This voltage is then quantized according to the ADC input voltage range V_h-V_l and bit depth b, giving the digital image output S.

$$\boldsymbol{S} = \frac{2^b - 1}{V_h\text{-}V_l}\left(\boldsymbol{O}_{CPN} + G_{FPGA}G_{SN}(\boldsymbol{E})\right) \qquad (4)$$

Data Sources: At the time of writing, the PanCam Flight Model is yet to be calibrated, and so the complete set of variables required for simulation is not yet available. Instead, manufacturer supplied information, datasheets, and preliminary calibration results of available components have been collected.

Optics. A duplicate of the PanCam filter suite, consisting of all 22 filters, has undergone preliminary characterisation at Aberystwyth University. The spectral transmission across 8 angles of incidence have been measured at <1nm Δλ. A reconstruction algorithm has been developed to interpolate a smooth 3D surface over the dimensions of wavelength, angle and transmission, such that a dense transmission cube can be reconstructed of the filter response at the resolution required for eq. 1. Manufacturer supplied responses of the WAC lens assemblies have been interpolated under the same procedure.

Detector. A large number of variables are required to describe the sensor response function. The detailed Star 1000 datasheet [6] is used as a guide, in particular providing the photovoltaic response, allowing for fitting of eq. 3. Empirical data of the Star 1000 detector has been provided for comparison by DLR, obtained during the MASCOT camera calibration campaign [7], and also from characterisation of candidate detectors for HRC on PanCam.

Simulation: The simulation flow is illustrated in figure 1. A software implementation has been written in IDL in an object-oriented framework. This allows a user to evaluate individual components of the system by calling the associated function, and for noise sources to be toggled to assess contributions. Once complete, the simulation software will be publically available.

Use Cases: Scene radiances of uniform white light at stepped illumination levels have been used to produce a Photon Transfer Curve (PTC) [8] of the virtual camera system. The details extracted from the PTC, describing the camera characteristics, have been compared to the simulation parameter variables, with discrepancies quantifying the accuracy of the PTC method. It has been demonstrated that the conventional PTC method is not valid for the nonlinear case of the Star 1000 CMOS detector, and thus alternative calibration techniques have been identified in the literature [9].

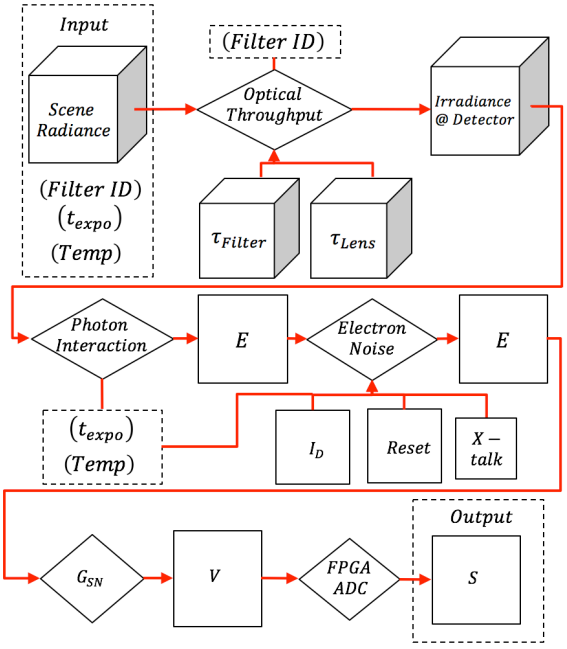

Fig 1. Block Diagram of the PanCam Wide Angle Camera simulation, describing the image chain from spectral scene radiance to digital image.

Future Work: The ability to analyze large batches of synthetic image sets will allow for detailed studies of image processing algorithms, where hardware data collection would otherwise be time and resource expensive. Already, the simulation has been used to assess and optimize auto-exposure algorithms; this will be extended to calibration and noise-reduction pipelines, and eventually to the information retrieval algorithms that will contribute to the PanCam science objectives during the ExoMars mission.

References: [1] Coates A. J. et al (2017) *Astrobiology, 17, 6-7,* 511-541. [2] Vago J. L. et al (2017) *Astrobiology*, *17*, *6-7*, 471-510. [3] Cousins C. R. et al (2012) *Plan. & Space Sci.*, *71*, 80-100 [4] Gunn M. & Cousins C. R. (2016) *Earth & Space Sci.*, *3, 4,* 144-162 [5] Gow R. D. et al (2007) *IEEE Trans. Elec. Dev., 54, 6,* 1321-1329. [6] On-Semiconductor (2015) *NOIS1SM1000 A/D* Star 1000 datasheet. [7] Jaumann et al (2016) *Space Sci. Rev., 208, 1-4,* 375-400 [8] Janesick J. (2007) *Photon Transfer, SPIE,* PM170.

Acknowledgements: This research has been funded by a UK Space Agency Aurora Studentship.